Supplemental material

Tanaka et al., https://doi.org/10.1084/jem.20181078

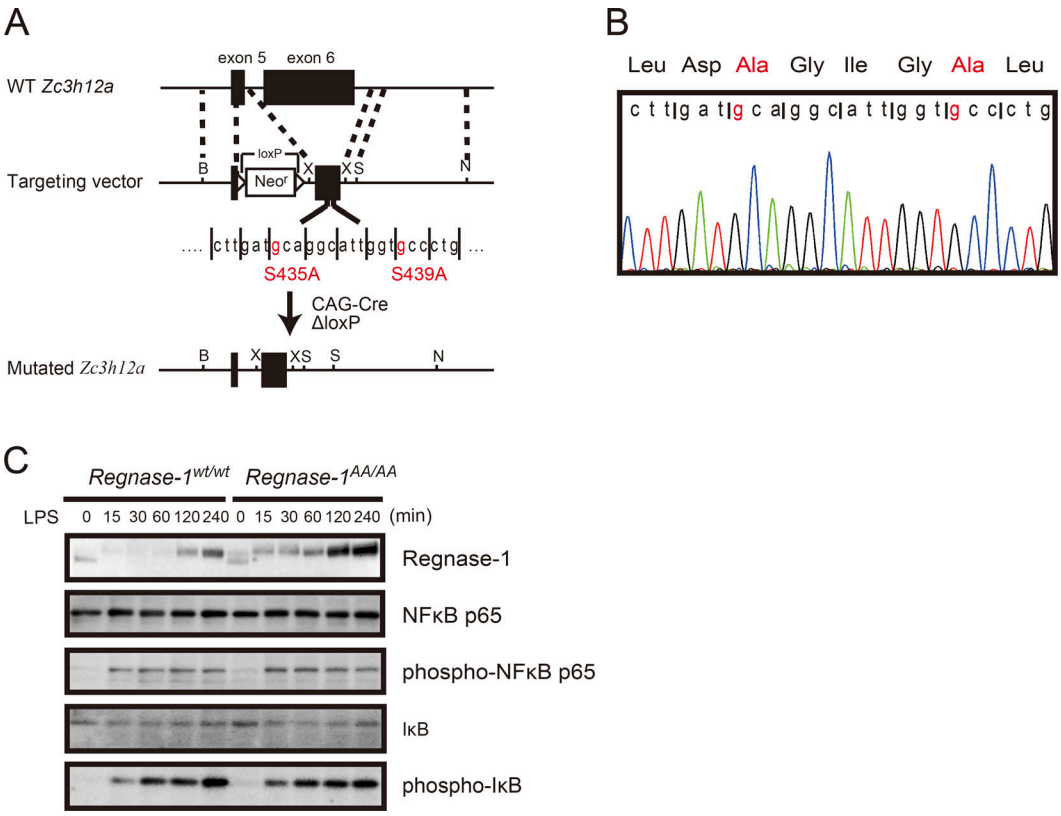

Figure S1. **Regnase-1 S435A/S439A (AA) knock-in mutation exerts resistance to IKK-mediated degradation. (A and B)** Generation of Regnase-1 S435A/S439A double knock-in (*Regnase-1*$^{AA/AA}$) mice. **(A)** Schematic view of WT *Regnase-1* gene (top), targeting vector (middle), and predicted mutated allele (bottom). Targeting vector contains S435A and S439A mutations in exon 6. NEO^r, neomycin resistance gene cassette. **(B)** Sequencing of *Regnase-1* exon 6 in the *Regnase-1*$^{AA/AA}$ mouse genome. Sequence chromatogram indicates replacement of TCA and TCC of Ser435 and Ser439 by GCA and GCC, respectively. **(C)** Immunoblotting analysis of Regnase-1, NF-κB, phosphor–NF-κB, IκB, and phospho-IκB in WT and *Regnase-1*$^{AA/AA}$ macrophages stimulated with LPS (100 ng/ml) for 0–240 min.

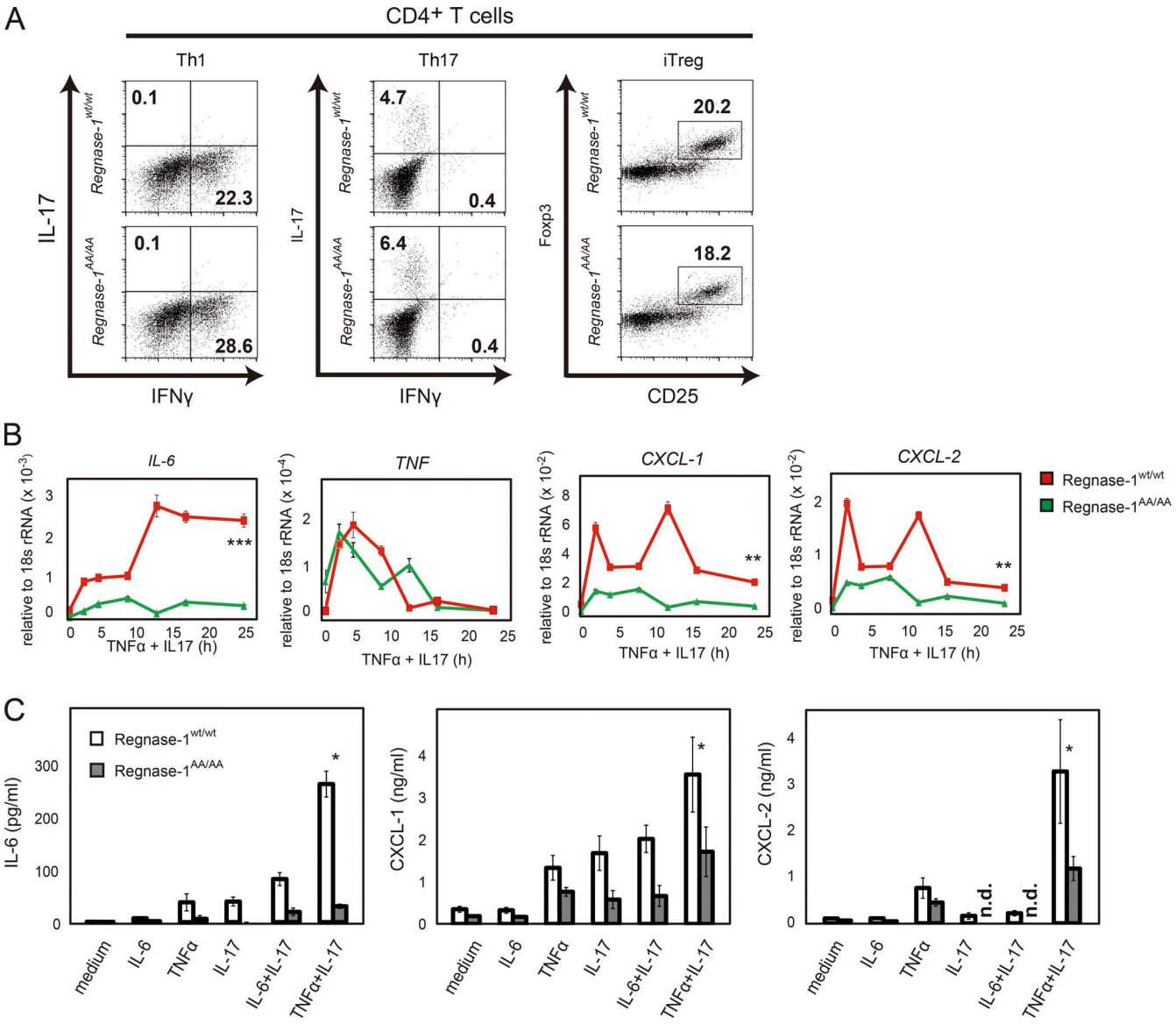

Figure S2. ***Regnase-1$^{AA/AA}$* mutation attenuates EAE disease severity through suppression of inflammatory response in nonhematopoietic cells.** **(A)** Flow cytometry analysis of CD4$^+$ T cell subsets (Th1, Th17, and iTreg) differentiated from naive CD4$^+$ T cells in vitro. **(B)** Quantitative PCR analysis of *IL-6*, *TNF-α*, *CXCL-1*, and *CXCL2* mRNA in WT and *Regnase-1$^{AA/AA}$* LSECs. Cells were stimulated with TNF-α (20 ng/ml) and IL-17A (50 ng/ml) for 0–24 h. Data were collected from four independent experiments. **, P < 0.01; ***, P < 0.005. **(C)** Production of IL-6, CXCL-1, and CXCL-2 by mouse LSECs in response to exposure to IL-6 (20 ng/ml), TNF-α (20 ng/ml), IL-17A (50 ng/ml), IL-6+IL-17A, or TNF-α+IL-17A for 24 h. Protein levels in cell supernatants were assessed by ELISA. Data were collected from three independent experiments. *, P < 0.05. rRNA, ribosomal RNA; iTreg, induced regulatory T; n.d., no difference.

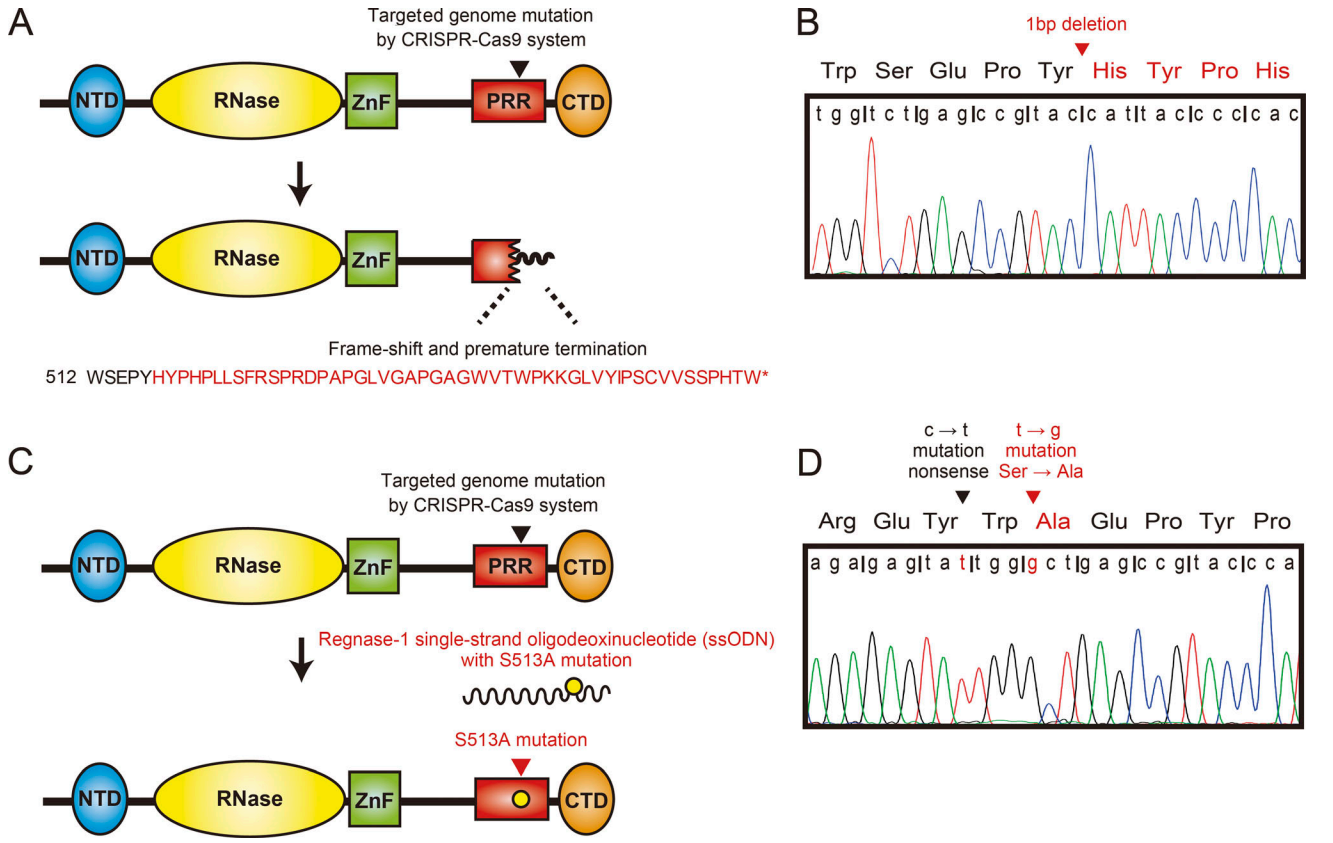

Figure S3. **Construction of Regnase-1 C-terminally truncated mutant mice (*Regnase-1 ΔCTD* mutant) with a 1-bp deletion that causes frameshift and the C-terminal truncation. (A)** Schematic view of WT Regnase-1 (top) and 1-bp truncated Regnase-1 (bottom). CRISPR/Cas9 targeting sites are located at the proline-rich region of Regnase-1. Amino acid sequences introduced by a frameshift mutation and a premature termination codon 146 bases downstream of the mutation are indicated in red. **(B)** Sequencing of *Regnase-1* exon 6 in the mouse genome mutated by CRISPR/Cas9. Sequence chromatogram indicates deletion of the cytosine base at Pro517 to initiate the frameshift mutation. **(C)** Schematic view of WT Regnase-1 (top) and S513A mutant of Regnase-1 (bottom). CRISPR/Cas9 targeting sites are located at Ser513 of Regnase-1. S513A mutation is introduced by coinjection of CRISPR/Cas9 targeting vector and single-strand oligodeoxynucleotide (ssODN) containing Regnase-1 exon sequence with S513A mutation. **(D)** Sequencing of *Regnase-1* exon 6 in the mouse genome mutated by CRISPR/Cas9. Sequence chromatogram indicates replacement of TAC and TAT of Tyr511 and TCT and GCT of Ser513, respectively.

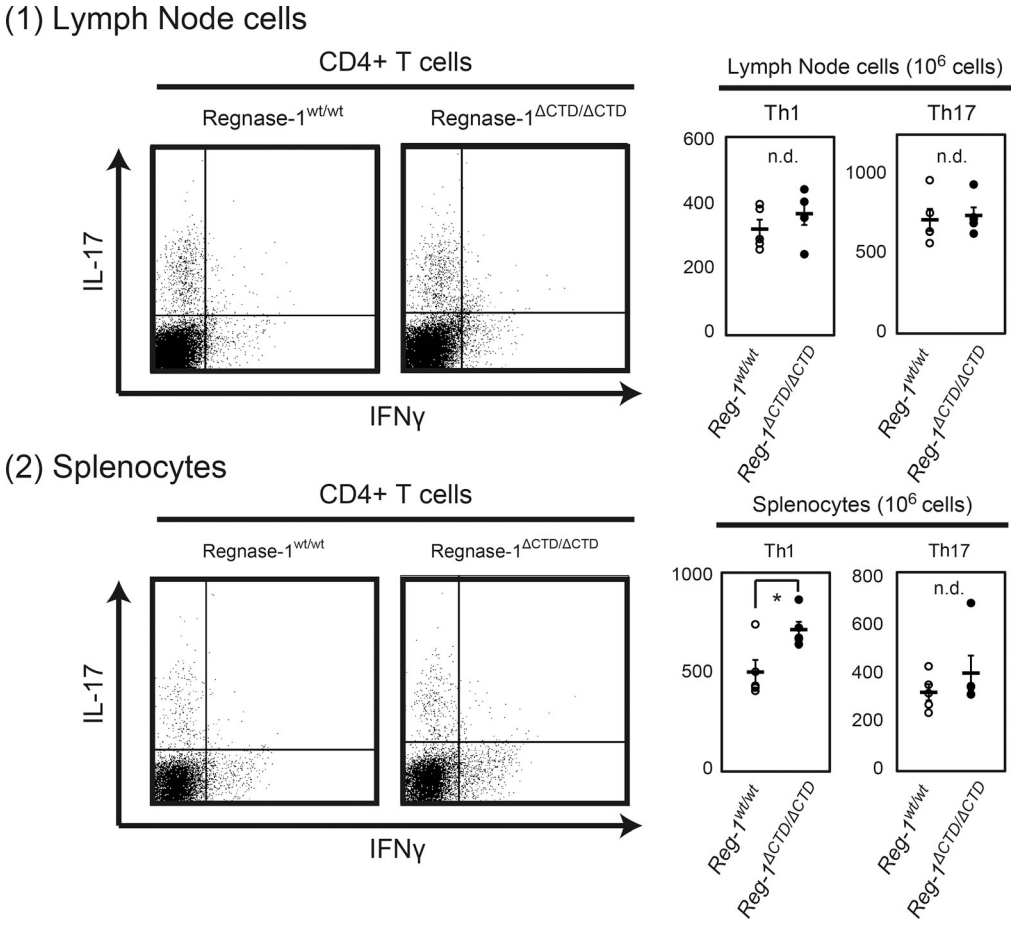

Figure S4. **Numbers of Th1 and Th17 cells are normal in lymph nodes but low in splenocytes from *Regnase-1 ΔCTD* mice with EAE pathogenesis.** Representative flow cytometric plots and statistics (each $n = 5$) of $CD4^+$ T cell subsets (Th1 and Th17) in lymph node cells (1.0×10^6 cells; 1) and splenocytes (1.0×10^6 cells; 2) from WT and *Regnase-1*$^{\Delta CTD/\Delta CTD}$ mice at 28 d after EAE immunization. *, $P < 0.05$. n.d., no difference.

Table S1. **Phosphorylation sites of Regnase-1 mediated by Act-1 and TBK1/IKKi**

Coexpression vectors in HEK293 cells	Regnase-1 only (control)	Regnase-1 + Act-1 + TBK1	Regnase-1 + Act-1 + IKKi
Sites identified only in control	Ser18, Ser68, Thr195, Ser299, Ser408, Thr522, Thr555	—	—
Sites commonly identified	Ser103, Ser114, Ser344, Thr348, Ser354, Ser359, Ser368, Ser374, Ser394, Ser454, Ser482	Ser103, Ser114, Ser344, Thr348, Ser359, Ser368, Ser374, Ser394, Ser454, Ser482	Ser103, Ser114, Ser344, Thr348, Ser368, Ser394, Ser394, Ser454
Sites identified only in both TBK-1 and IKKi	—	Ser28, Ser124, Thr115, Ser288, Ser494, Ser508, Ser513	
Sites identified only in TBK-1	—	Thr109, Ser404, Ser454, Ser470, Ser482, Thr498, Thr505, Ser592,	—
Sites identified only in IKKi	—	—	Ser21, Ser268, Ser386, Ser439, Ser474